

# Geophysical Research Letters

## RESEARCH LETTER

10.1029/2018GL080475

### Key Points:

- New quasi-annual  $^{10}\text{Be}$  data were taken with Antarctic Dome Fuji ice core over the period when the 994-CE cosmic ray event took place
- We observed a ~50% increase in  $^{10}\text{Be}$  concentrations, which is consistent with the  $^{10}\text{Be}$  increases observed in the Greenland ice cores
- We propose a phenomenological method for evaluating a common deposition component between quasi-annual beryllium-10 data and  $\text{Na}^+$  data

### Supporting Information:

- Supporting Information S1
- Data Set S1

### Correspondence to:

F. Miyake,  
fmiyake@isee.nagoya-u.ac.jp

### Citation:

Miyake, F., Horiuchi, K., Motizuki, Y., Nakai, Y., Takahashi, K., Masuda, K., et al. (2019).  $^{10}\text{Be}$  signature of the cosmic ray event in the 10th century CE in both hemispheres, as confirmed by quasi-annual  $^{10}\text{Be}$  data from the Antarctic Dome Fuji ice core. *Geophysical Research Letters*, 46, 11–18. <https://doi.org/10.1029/2018GL080475>




Received 17 SEP 2018

Accepted 14 DEC 2018

Accepted article online 18 DEC 2018

Published online 8 JAN 2019

## $^{10}\text{Be}$ Signature of the Cosmic Ray Event in the 10th Century CE in Both Hemispheres, as Confirmed by Quasi-Annual $^{10}\text{Be}$ Data From the Antarctic Dome Fuji Ice Core

F. Miyake<sup>1</sup> , K. Horiuchi<sup>2</sup>, Y. Motizuki<sup>3</sup>, Y. Nakai<sup>3</sup> , K. Takahashi<sup>3</sup>, K. Masuda<sup>1</sup>, H. Motoyama<sup>4</sup> , and H. Matsuzaki<sup>5</sup>

<sup>1</sup>Institute for Space-Earth Environmental Research, Nagoya University, Nagoya, Japan, <sup>2</sup>Graduate School of Science and Technology, Hirosaki University, Hirosaki, Japan, <sup>3</sup>RIKEN Nishina Center, Wako, Japan, <sup>4</sup>National Institute of Polar Research, Tokyo, Japan, <sup>5</sup>MALT, The University Museum, The University of Tokyo, Tokyo, Japan

**Abstract** Cosmogenic nuclides are good indicators of past cosmic ray events and variations. To verify such phenomena, it is important to evaluate them using multiple nuclides from different archives. The cosmic ray event in 993–994 Common Era (CE) has already been confirmed with  $^{14}\text{C}$  and  $^{10}\text{Be}$  data, which show rapid increases in the concentrations. However, the  $^{10}\text{Be}$  data were obtained from the Greenland ice cores in the Northern Hemisphere. To investigate the extent of the  $^{10}\text{Be}$  increase in the Southern Hemisphere, we measured quasi-annual  $^{10}\text{Be}$  concentrations between 980 and 1,011 CE in the Antarctic Dome Fuji ice core. We observed a ~50% increase in  $^{10}\text{Be}$  concentration around 994 CE, consistent with the Greenland data. Increases in  $^{10}\text{Be}$  concentrations in both hemispheres support a solar origin of the 994-CE event. In addition, we propose a method of evaluating the so-called “system effect” for  $^{10}\text{Be}$  deposition by extracting common components from  $^{10}\text{Be}$  and  $\text{Na}^+$  data.

**Plain Language Summary** New quasi-annual beryllium-10 measurements were made with the Dome Fuji ice core from Antarctica over the period in which the 994 cosmic ray event would be expected. We observed an approximately 50% increase in beryllium-10 concentrations, which is consistent with the beryllium-10 increases observed in the Greenland ice cores. This lends support to a solar origin of the 994 event. We propose a phenomenological method for evaluating a common deposition component between quasi-annual beryllium-10 and sodium ion data.

## 1. Introduction

Two rapid increases in  $^{14}\text{C}$  concentrations, the first occurring in 774–775 Common Era (CE) and the second in 993–994 or 992–993 CE (hereafter referred to as the 775 event and the 994 event), were first detected in Japanese tree rings. The 775 event was identified even in the decadal  $^{14}\text{C}$  data (INTCAL) and  $^{10}\text{Be}$  data (Dome Fuji [DF] ice core) as a rapid change (Usoskin & Kovaltsov, 2012). The 775 and 994 events were confirmed by subsequent independent annual  $^{14}\text{C}$  measurements using worldwide tree samples (Büntgen et al., 2018; Fogtmann-Schulz et al., 2017; Gütler et al., 2015; Jull et al., 2014; Miyake et al., 2012, 2013, 2014; Park et al., 2017; Rakowski et al., 2015; Usoskin et al., 2013; Uusitalo et al., 2018). Carbon-14 is a nuclide produced by cosmic rays (CR), which are high energy particles with origins in outside the solar system (Galactic CR: GCR) or an eruption of the sun (Solar Energetic Particles). The increases in  $^{14}\text{C}$  concentrations in 775 and 994 CE point to an extraterrestrial event that induced CR incident on the Earth within 1 year.

Information from other cosmogenic nuclides, such as  $^{10}\text{Be}$  and  $^{36}\text{Cl}$ , becomes important in a discussion of the origin of the 775 and 994 events, because a ratio of cosmogenic nuclide production rates varies depending on the types and energies of incident particles. Several studies have reported  $^{10}\text{Be}$  and  $^{36}\text{Cl}$  data from Greenland and Antarctic ice cores around the 775 event (Mekhaldi et al., 2015; Miyake et al., 2015; Sigl et al., 2015). Quasi-annual  $^{10}\text{Be}$  data were taken from ice cores of the North Greenland Ice Core Project (NGRIP), North Greenland Eemian Ice Drilling (NEEM), and TUNU2013 in Greenland and the West Antarctic Ice Sheet Divide Ice Core and DF in Antarctica. All of the ice cores showed sharp  $^{10}\text{Be}$  increases that corresponded with the 775 event with a dating uncertainty in the original age model of ice cores of

$\pm 7$  years (Mekhaldi et al., 2015; Miyake et al., 2015; Sigl et al., 2015). A sharp  $^{36}\text{Cl}$  peak was also detected in the GRIP core, although the time resolution was not quasi-annual but approximately 5 years (Mekhaldi et al., 2015; Wagner et al., 2000). Using data from these cosmogenic nuclides, Mekhaldi et al. (2015) concluded the origin of the events was an extreme Solar Proton Event (SPE) or several SPEs, whose energy spectrum is very hard compared to the SPE of 2005 CE. Sukhodolov et al. (2017) modeled the 775 event as the scaled SPE signal using  $^{10}\text{Be}$  data from four ice core sites.

On the other hand, quasi-annual data from cosmogenic nuclides other than  $^{14}\text{C}$  in association with the 994 event are still very limited. Only a few  $^{10}\text{Be}$  data sets have been published. The data sets were collected from the NGRIP and NEEM sites in Greenland, and they showed small  $^{10}\text{Be}$  increases of  $\sim 50\%$  over background levels relative to 775 CE (Mekhaldi et al., 2015). Although the  $^{10}\text{Be}$  peaks associated with the 994 event were small and comparable to background, the event could be explained by an extreme SPE with a hard energy spectrum, since  $^{14}\text{C}$  and  $^{10}\text{Be}$  production agreed within the margin of error (Mekhaldi et al., 2015). The  $^{14}\text{C}$  data indicate the amplitude of the 994 event was half of the 775 event (Büntgen et al., 2018). If the 994 and 775 events shared the same origin, the increase in  $^{10}\text{Be}$  concentration corresponding to the 994 event would also be smaller than that observed for the 775 event.

The difficulty in identifying such a small  $^{10}\text{Be}$  signal may be one of the reasons behind the limited number of publications related to quasi-annual  $^{10}\text{Be}$  data for the 994 event. Such a small signal could be disturbed easily by the so-called “system effect,” which is related to  $^{10}\text{Be}$  transport and deposition processes (Abreu et al., 2013; Steinhilber et al., 2012). Indeed, the larger  $^{10}\text{Be}$  peak in our previous study, which was associated with the 775 event (Miyake et al., 2015), was superimposed on a background in which variation in the  $^{10}\text{Be}$  signal was synchronous with variation in the  $\text{Na}^+$  signal. Baroni et al. (2011) also reported a positive correlation between signals from  $^{10}\text{Be}$  and  $\text{Na}^+$ , as well as those from other ions of sea-salt origin, in quasi-annual data from inland Antarctica. They argued the correlation reflected a troposphere-modulated contribution to  $^{10}\text{Be}$  variation. Although the cause of this correlation has not been fully elucidated, it is possible that the similarities in  $^{10}\text{Be}$  and  $\text{Na}^+$  behavior have been attributed to the system effect. If we could evaluate correlations between signals of  $^{10}\text{Be}$  and other species that are unrelated to the original CR variations, we could view the CR information more clearly. Therefore, it is important to investigate the relationships between  $^{10}\text{Be}$  and other species, such as  $\text{Na}^+$ , to establish a method for evaluating the system effect.

Although it has been proposed that the origin of the 994 event was an extreme SPE, investigations of the ratio of  $^{14}\text{C}$  and  $^{10}\text{Be}$  production rates have only considered  $^{10}\text{Be}$  data obtained from ice cores collected in the Northern Hemisphere. In this study, we analyzed  $^{10}\text{Be}$  concentrations in an ice core from the DF station around the 994 event at a quasi-annual resolution to determine whether a similar  $^{10}\text{Be}$  signal could be found in the Antarctic ice core. If we detected a comparable  $^{10}\text{Be}$  signal in the DF data, it would mean that CR incident on the Earth entered nearly isotropically. This scenario would favor a solar proton origin, which would be affected by geomagnetic fields. In addition, we investigated the commonalities between  $^{10}\text{Be}$  and  $\text{Na}^+$  collected from the same ice core. Finally, we devised a phenomenological method for evaluating the common system effect from the quasi-annual record of cosmogenic  $^{10}\text{Be}$ .

## 2. Materials and Methods

### 2.1. DF01 Core and Its Chronologies

We used the DF01 core, a shallow ice core drilled at the DF station in 2001. The DF01 core is stored at National Institute of Polar Research as an ice core section with cuts every 50 cm (supporting information Figure S1). The DF station is located near the highest point of Dronning Maud Land ( $77^{\circ}19'\text{S}$ ,  $39^{\circ}42'\text{E}$ ), 3,810 m above sea level. It has been suggested that inland snow precipitations in Antarctica, including those at the DF site, hold more stratospheric information than the tropospheric information compared with the coastal regions of Antarctica (Fourré et al., 2006).

It was difficult to date the DF01 core using the annual layer counting method, since the snow accumulation rate in the DF region is very low and shows little seasonal variation. For example, snow accumulation rates averaged over 741 and 7,100 years were  $25.2 \pm 0.3$  and  $25.0 \pm 1.3 \text{ kg}\cdot\text{m}^{-2}\cdot\text{year}^{-1}$ , respectively (Fujita et al., 2011; Igarashi et al., 2011). Hence, the age of the DF01 core has been estimated by  $^{10}\text{Be}$ - $^{14}\text{C}$  matching and volcanic tie point matching. With these methods, the following chronologies of the DF01 core were

independently determined: (1) the  $^{10}\text{Be}$ - $^{14}\text{C}$  age (Horiuchi et al., 2008); (2) the DFS1 chronology; and (3) the DFS2 chronology (Motizuki et al., 2014). The  $^{10}\text{Be}$ - $^{14}\text{C}$  age was constructed mainly by  $^{10}\text{Be}$ - $^{14}\text{C}$  matching in which  $^{10}\text{Be}$  data obtained from quasi-decadal measurements of each core section were compared to  $^{14}\text{C}$  production rates calculated using the INTCAL  $^{14}\text{C}$  data with decadal time resolution (Stuiver et al., 1998; Usoskin & Kromer, 2005). The  $^{10}\text{Be}$  and  $^{14}\text{C}$  data used for matching had 10-year resolution, and the resulting chronology was quasi-decadal. The DFS1 and the DFS2 chronologies were constructed by volcanic tie point matching. Motizuki et al. (2014) identified the volcanic events through analysis of nonsea salt sulfate (nss  $\text{SO}_4^{2-}$ ) in the divided section cores with an average time resolution of 0.9 years. The volcanic signal appeared as spikes in nss  $\text{SO}_4^{2-}$  concentrations. Since the closest volcanic tie points are 686 and 1,108 CE (DFS1) and 694 and 1,170 CE (DFS2), the 994 event can be a time marker where a section of more than 400 years with no volcanic markers if we detected the 994 spike in the DF core. Not only nss  $\text{SO}_4^{2-}$  but also other ion species have been analyzed in the same DF01 cores with the same time resolution (Motizuki et al., 2017).

## 2.2. Selection of Core Sections of DF01

In our previous analysis of the 775 event (Miyake et al., 2015), we selected sections in the DF01 core based on their  $^{10}\text{Be}$ - $^{14}\text{C}$  ages (Horiuchi et al., 2008) and detected a sharp  $^{10}\text{Be}$  increase corresponding to the 775 event. The difference between the  $^{10}\text{Be}$ - $^{14}\text{C}$  age and the tree-ring age around the 775 event is about 5 years only (Miyake et al., 2015). Thus, the  $^{10}\text{Be}$ - $^{14}\text{C}$  age method successfully determined the ice core age with acceptable accuracy.

The approach used in our analysis of the 775 event was applied in the present study. First, we estimated the age of the ice-core sections by the  $^{10}\text{Be}$ - $^{14}\text{C}$  age method. Based on their  $^{10}\text{Be}$ - $^{14}\text{C}$  age, the ice core sections around 994 CE were numbered DF01 #103–#105, corresponding to 1,005–985 CE. Since we identified a sharp  $^{10}\text{Be}$  peak in the #104 section, which represented the second-largest increase in the  $^{10}\text{Be}$  concentration in quasi-decadal data from 695 to 1,005 CE (note: the largest  $^{10}\text{Be}$  peak for the same interval coincided with the 775 event; Horiuchi et al., 2007, 2008), it is possible the  $^{10}\text{Be}$  signal detected in the #104 section is attributable to the 994 event. The  $^{10}\text{Be}$ - $^{14}\text{C}$  ages of core sections #103–#105 were in good agreement with the DFS1 and DFS2 chronologies, falling within 3 and 5 years of their DFS1 and DFS2 ages, respectively. The close agreement between independent chronologies gave us confidence in the accuracy of our initial age determination for sections #103–#105, which included the 994 event. Table S1 gives information about the core sections, chronologies of the DF01 core, and the previously published quasi-decadal  $^{10}\text{Be}$  data.

## 2.3. Pretreatments and Measurement

We divided each core section into 10–12 samples for  $^{10}\text{Be}$  analysis (Table S1). Each length of division is the same as the previous nss  $\text{SO}_4^{2-}$  and other ion species measurements (Motizuki et al., 2014, 2017). The time resolution of the samples is a quasi-annual. Sample pretreatments were carried out at the Paleoenvironmental and Cosmogenic-Nuclide Laboratory, Hirosaki University, using a method (Miyake et al., 2015) modified from Horiuchi et al. (2007).  $^{10}\text{Be}$  analysis was performed as described by Miyake et al. (2015) on a 5 MV accelerator mass spectrometer at the University of Tokyo (Matsuzaki et al., 2007). Ion chromatography data from the DF01 core can be found in Motizuki et al. (2017).

## 3. Results

The quasi-annual data set of  $^{10}\text{Be}$  concentrations is plotted against the three independent chronologies for the DF01 core in Figure S2. Among these, the largest  $^{10}\text{Be}$  peak reflected a 51% increase above the average of the  $^{10}\text{Be}$  concentrations in 992.3 CE ( $^{10}\text{Be}$ - $^{14}\text{C}$  age), 994.5 CE (DFS1), and 998.3 CE (DFS2). Since the  $^{10}\text{Be}$  peak appears at year 994 ( $\pm 5$ ) CE in all the three chronologies, it is reasonable to conclude the peak reflects the 994 event and to identify the point as 994 CE. Figure 1 shows the  $^{10}\text{Be}$  profile plotted against a modified  $^{10}\text{Be}$ - $^{14}\text{C}$  age model, in which the time axis is shifted to align the  $^{10}\text{Be}$  peak to 994 CE. In the following, we use this age model for both  $^{10}\text{Be}$  and  $\text{Na}^+$  data obtained from the same core (Figure 1), referring to it as “tree-ring age.”

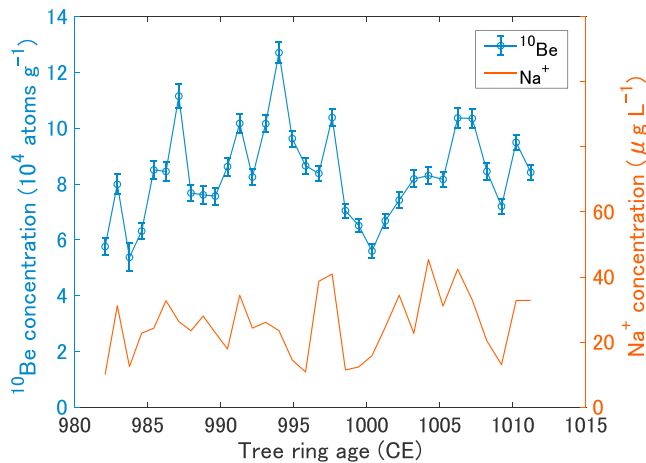


**Figure 1.** Comparison between  $^{10}\text{Be}$  and  $\text{Na}^+$  data around 994 CE. The horizontal line is shifted from the original  $^{10}\text{Be}$ - $^{14}\text{C}$  age model so that the largest  $^{10}\text{Be}$  peak to be 994 CE (see text). CE = Common Era.

Beryllium-10 is produced by a spallation reaction caused by CR in the atmosphere, primarily in the stratosphere and the upper troposphere (approximately 65% of  $^{10}\text{Be}$  atoms are produced in the stratosphere by GCR or more than 65% of  $^{10}\text{Be}$  atoms are produced by Solar Energetic Particles whose energy spectrum is softer than that of GCR; Heikkilä et al., 2013; Poluianov et al., 2016). It is believed that  $^{10}\text{Be}$  atoms react immediately with oxygen ( $^{10}\text{Be} + \text{O} \rightarrow ^{10}\text{BeO}$ ), attach to aerosols, and finally fall to the ground through atmospheric circulation and precipitation (Beer et al., 2012). There are many types of atmospheric aerosol particles, and most of them contain ionic species including  $\text{Na}^+$ . Although a mechanism causing positive correlation between  $^{10}\text{Be}$  and  $\text{Na}^+$  data has not been figured out, there is probably a common depositional process in these two species. Baroni et al. (2011) suggested the correlations between  $^{10}\text{Be}$  and other ion species could be explained by troposphere-modulated contributions, such as the Antarctic Oscillation or the Antarctic Circumpolar Wave. Although large atmospheric fluctuations such as the Antarctic Oscillation have not been confirmed yet as the main cause of the correlations, we can probably evaluate part of the system effect of  $^{10}\text{Be}$  using  $\text{Na}^+$  data.

#### 4.2. Evaluation of the System Effect Using $\text{Na}^+$ Data

Since positive correlation between  $^{10}\text{Be}$  and  $\text{Na}^+$  was confirmed in this study and in two other independent studies, it may be possible to use this correlation between  $^{10}\text{Be}$  and  $\text{Na}^+$  concentrations as an indicator of the system effect.

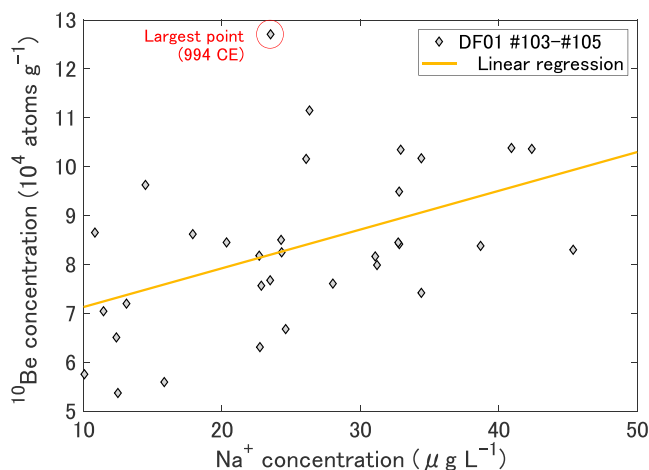


**Figure 2.** Relationship between  $\text{Na}^+$  and  $^{10}\text{Be}$  data. The circled data correspond to 994 CE in the tree-ring age. The correlation coefficient of the linear regression is  $R = 0.46$  ( $p = 0.0064$ ). If we omit the largest point, the correlation becomes improved ( $R = 0.54$ ). CE = Common Era; DF = Dome Fuji.

## 4. Discussions

### 4.1. Correlation Between $^{10}\text{Be}$ and $\text{Na}^+$

A positive correlation between annual  $^{10}\text{Be}$  data and  $\text{Na}^+$  data has been reported in previous studies of Antarctic Vostok and DF ice cores (Baroni et al., 2011; Miyake et al., 2015). The linear correlation coefficient ( $R$ ) between the two species for the last 60 years at Vostok was 0.51 (Baroni et al., 2011).  $R = 0.49$  circa 775 CE (763–794 CE) at DF (Miyake et al., 2015). In addition, Baroni et al. (2011) reported a similar correlation between  $^{10}\text{Be}$  concentrations and those of some other chemical species of marine (sea salt) origin, for example, sea-salt sulfate and magnesium, in quasi-annual data. We checked our  $^{10}\text{Be}$  and  $\text{Na}^+$  data obtained from the same core (Motizuki et al., 2017) for similar correlations. Our findings were consistent with those of previous studies; we found a weak correlation ( $R = 0.46$ ;  $t = 2.9$ ,  $p = 0.007$ ) between  $^{10}\text{Be}$  and  $\text{Na}^+$  (Figure 2).

Beryllium-10 is produced by a spallation reaction caused by CR in the atmosphere, primarily in the stratosphere and the upper troposphere (approximately 65% of  $^{10}\text{Be}$  atoms are produced in the stratosphere by

GCR or more than 65% of  $^{10}\text{Be}$  atoms are produced by Solar Energetic Particles whose energy spectrum is softer than that of GCR; Heikkilä et al., 2013; Poluianov et al., 2016). It is believed that  $^{10}\text{Be}$  atoms react immediately with oxygen ( $^{10}\text{Be} + \text{O} \rightarrow ^{10}\text{BeO}$ ), attach to aerosols, and finally fall to the ground through atmospheric circulation and precipitation (Beer et al., 2012). There are many types of atmospheric aerosol particles, and most of them contain ionic species including  $\text{Na}^+$ . Although a mechanism causing positive correlation between  $^{10}\text{Be}$  and  $\text{Na}^+$  data has not been figured out, there is probably a common depositional process in these two species. Baroni et al. (2011) suggested the correlations between  $^{10}\text{Be}$  and other ion species could be explained by troposphere-modulated contributions, such as the Antarctic Oscillation or the Antarctic Circumpolar Wave. Although large atmospheric fluctuations such as the Antarctic Oscillation have not been confirmed yet as the main cause of the correlations, we can probably evaluate part of the system effect of  $^{10}\text{Be}$  using  $\text{Na}^+$  data.

Since positive correlation between  $^{10}\text{Be}$  and  $\text{Na}^+$  was confirmed in this study and in two other independent studies, it may be possible to use this correlation between  $^{10}\text{Be}$  and  $\text{Na}^+$  concentrations as an indicator of the system effect. Thus, we made the following simplifying assumptions regarding the source of variations in  $^{10}\text{Be}$  and  $\text{Na}^+$  concentrations: (1) variations in  $^{10}\text{Be}$  concentrations are caused by a combination of the system effect and a production effect caused by CR; and (2) variations in  $\text{Na}^+$  concentrations are caused mainly by the common system effect with  $^{10}\text{Be}$ . If we eliminate the common signal between  $^{10}\text{Be}$  and  $\text{Na}^+$  from the original  $^{10}\text{Be}$  concentration data, information related to the production of  $^{10}\text{Be}$  should be identifiable.

We can obtain relative production variability of  $^{10}\text{Be}$  information, henceforth called  $\Delta^{10}\text{Be}(t)$ , from the difference between the  $^{10}\text{Be}$  data and a regression line constructed with the  $^{10}\text{Be}$  and  $\text{Na}^+$  concentration data as shown in equation (1),

$$\Delta^{10}\text{Be}(t) = ^{10}\text{Be}(t) - C(\text{Na}(t)), \quad (1)$$

where  $^{10}\text{Be}(t)$  is the normalized  $^{10}\text{Be}$  concentration,  $\text{Na}(t)$  is the normalized  $\text{Na}^+$  concentration, and  $C(t)$  is the regression line between the normalized  $^{10}\text{Be}$  and  $\text{Na}^+$  concentrations. Figure 3a shows the normalized  $^{10}\text{Be}$  and  $\text{Na}^+$  concentrations, and Figure 3b shows  $\Delta^{10}\text{Be}(t)$ .

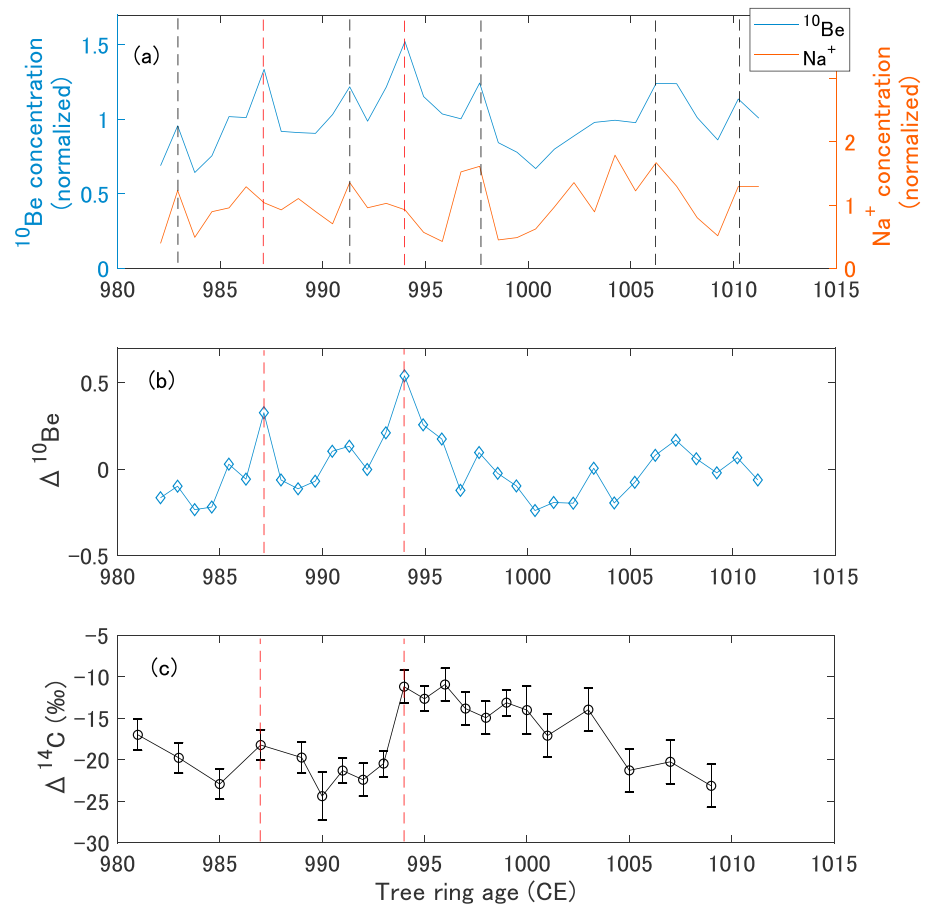


**Figure 3.** (a) Comparison between  $^{10}\text{Be}$  and  $\text{Na}^+$  data around 994 CE. While several  $^{10}\text{Be}$  peaks are accompanied by  $\text{Na}^+$  peaks (black broken lines), there are no  $\text{Na}^+$  peaks corresponding to the largest  $^{10}\text{Be}$  peak in 994 CE and the second largest  $^{10}\text{Be}$  peak in 987 CE (red broken lines). (b)  $\Delta^{10}\text{Be}$  values whose calculation method is provided in the text. (c)  $\Delta^{14}\text{C}$  values from Japanese tree rings (Miyake et al., 2013). CE = Common Era.

### 4.3. The 994 CE CR Event

Figure 3a reveals similarities in the characteristic variations of  $^{10}\text{Be}$  and  $\text{Na}^+$  concentrations. Several  $^{10}\text{Be}$  increases are accompanied by corresponding increases in  $\text{Na}^+$ . However, the largest and second-largest peaks in  $^{10}\text{Be}$  concentration, corresponding to 994 and 987 CE (tree-ring age), are not accompanied by  $\text{Na}^+$  peaks. As Figure 1 shows, this is consistent with the original  $^{10}\text{Be}$  and  $\text{Na}^+$  data. This makes the two  $^{10}\text{Be}$  peaks emphasized in the  $\Delta^{10}\text{Be}$  profile (Figure 3b). For example, the increment of the largest peak against the standard deviation of the  $\Delta^{10}\text{Be}$  data excluding the largest peak is 3.7, whereas that of the original  $^{10}\text{Be}$  data is 3.0.

Quasi-annual and quasi-semiannual  $^{10}\text{Be}$  data around the 994 event were collected in previous measurements of the Greenland cores (NEEM and NGRIP). We compared this  $^{10}\text{Be}$  data with ours in Figure 4. The time resolutions of the NEEM and NGRIP data were quasi-semiannual and quasi-annual, respectively (Mekhaldi et al., 2015; Sigl et al., 2015). In addition, we compared the NEEM average annual resolution data to the DF and NGRIP data. The horizontal axes in Figure 4 are shifted to align the largest  $^{10}\text{Be}$  point with 994 CE. The offsets from the original ice core ages are +1.7 years from the  $^{10}\text{Be}$ - $^{14}\text{C}$  age (this study), +5.4 years (Mekhaldi et al., 2015), and +7 years (Sigl et al., 2015). The largest peak in the annually resolved NEEM data set represents a 52% increase in  $^{10}\text{Be}$  concentration above the average for the data set. The largest peak in the NGRIP data set represents an increase of 41% in  $^{10}\text{Be}$  concentration above average. These values are nearly equal to the increase found in the DF data (51%). These  $^{10}\text{Be}$  increments above the averages indicate an additional  $^{10}\text{Be}$  production against the normal production mainly by GCR. Then the consistency of

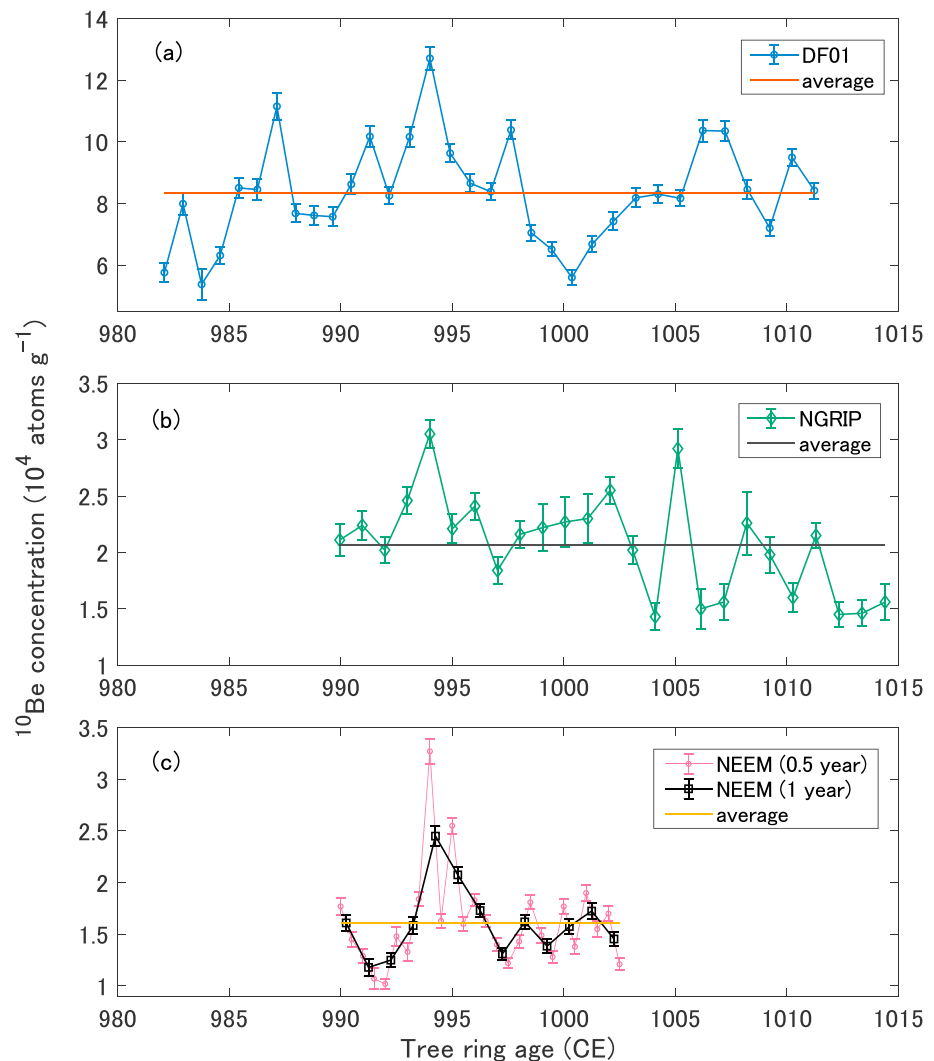


**Figure 4.**  $^{10}\text{Be}$  concentration data from both hemispheres around 994 CE. (a) Circles show measured quasi-annual data from Antarctic DF. The line shows an average of the data ( $8.3 \times 10^4$  [atoms  $\text{g}^{-1}$ ]). (b) Quasi-annual measurements of the Greenland ice cores from the NGRIP shown in diamonds (Mekhaldi et al., 2015). The line shows an average of the data ( $2.1 \times 10^4$  [atoms  $\text{g}^{-1}$ ]). The horizontal line is shifted +5.4 years to the original ice core age the Greenland Ice Core Chronology 2005 bottom to the largest point to be 994 CE. (c)  $^{10}\text{Be}$  data (0.5- and 1-year time resolutions) of the NEEM core from Greenland (Sigl et al., 2015). The line shows average of all data ( $1.6 \times 10^4$  [atoms  $\text{g}^{-1}$ ]). The corrected age indicates an original ice core age +7 years to match the  $^{10}\text{Be}$  peak with 994 CE (Sigl et al., 2015). CE = Common Era; DF = Dome Fuji; NEEM = North Greenland Eemian Ice Drilling; NGRIP = North Greenland Ice Core Project.

the increments between both hemispheres implies almost equal  $^{10}\text{Be}$  production was occurred in both hemispheres.

The  $^{10}\text{Be}$  peaks in Greenland data considered to correspond to the 994 event by Mekhaldi et al. (2015) are not readily distinguished from background variation (Figure 4). The increase around 1,005 CE in the NGRIP core is more rapid and is greater in magnitude than the change occurring around 994 CE, and this is also same in the estimated  $^{10}\text{Be}$  flux data (Mekhaldi et al., 2015). However, nearly identical  $^{10}\text{Be}$  increases are observed in three independent records from both hemispheres at the expected age. Therefore, it is possible that the ~50% increase in  $^{10}\text{Be}$  concentration was caused by the 994 event. This also means that  $^{10}\text{Be}$  increases identified in both hemispheres related to the 775 and 994 events were similar but a factor ~1.5 difference in magnitude. This is consistent with extreme SPE origin, of the 994 event, which has been proposed by Mekhaldi et al. (2015).

Figure 3c shows  $^{14}\text{C}$  data obtained from a Japanese cedar tree sample (Miyake et al., 2013) around the 994 event. In addition to a  $^{14}\text{C}$  concentration increase in 994 CE, there is also a small  $^{14}\text{C}$  increase from 985 to 987 CE (tree-ring age), which corresponds to the second-largest  $^{10}\text{Be}$  peak in our DF data. This small  $^{14}\text{C}$  peak represents a 4.7‰ increase in  $\Delta^{14}\text{C}$  and is 2.5 times larger than the measurement error. It is possible that the second-largest peak reflects a CR variation. However, the details of  $^{14}\text{C}$  variation are unknown, because the  $^{14}\text{C}$  data around the second peak are biannually resolved. Fogtmann-Schulz et al. (2017) measured  $^{14}\text{C}$  concentrations for the period 980–1,006 CE with annual resolution. Although no  $^{14}\text{C}$  increase was identified around 987 CE, the data from 985 to 987 CE were only taken in the late wood. Additional high-precision and high-time-resolution  $^{14}\text{C}$  measurements are necessary to determine whether a rapid CR increase also occurred around 987 CE.

## 5. Conclusions and Final Remarks

We measured quasi-annual  $^{10}\text{Be}$  concentrations in the DF01 core for the period from 980 to 1,011 CE based on the  $^{10}\text{Be}$ - $^{14}\text{C}$  age (#103–#105 core sections), where evidence of the CR event in 994 CE would be expected. We detected the largest  $^{10}\text{Be}$  increase, indicated by a peak of ~50% above baseline, in 992.3 CE ( $^{10}\text{Be}$ - $^{14}\text{C}$  age). Since the increase in  $^{10}\text{Be}$  concentration was identified in three independent chronologies of the DF01 core around 994 CE (992–998 CE), it is possible that the  $^{10}\text{Be}$  peak corresponds to the 994-CE event. Hence, we propose the  $^{10}\text{Be}$  peak may be used as a time marker for 994 CE.

In addition, we found a correlation between  $^{10}\text{Be}$  and  $\text{Na}^+$  concentrations in the same ice cores, in agreement with the results of previous studies. Since both of the species are related to aerosol deposition in the atmosphere, we interpret this correlation as indication, at least partly, of the system effect on  $^{10}\text{Be}$  deposition. Based on this interpretation, we evaluated the system effect using a common component in the  $^{10}\text{Be}$  and  $\text{Na}^+$  data. Consequently, the  $^{10}\text{Be}$  peak in 994 CE became more significant relative to background.

Since a positive correlation between quasi-annual  $^{10}\text{Be}$  and  $\text{Na}^+$  concentrations has been identified in all the annual measurement data from the DF core so far (Miyake et al., 2015; this study), the correlation between the two species might be observed in annual data from the DF core through at least the Holocene epoch, where no evidence of drastic climate change has been reported (e.g., Kawamura et al., 2017; Uemura et al., 2018). We propose a part of the so-called system effect in quasi-annual  $^{10}\text{Be}$  data can be phenomenologically evaluated with  $\text{Na}^+$  data from the same core. Although the correlation between  $^{10}\text{Be}$  and  $\text{Na}^+$  is found, its cause has not been elucidated. In the future, it will be necessary to reveal its cause by investigating productions, transportation processes, and chemical dynamics of these species and other ionic species such as  $\text{SO}_4^{2-}$ .

The ~50% increase in  $^{10}\text{Be}$  concentration in the DF core is consistent with  $^{10}\text{Be}$  data obtained from the Greenland NEEM and NGRIP cores. Nearly equal increases in  $^{10}\text{Be}$  detected in both hemispheres support an extreme SPE origin of the 994 event. Another weaker  $^{10}\text{Be}$  peak was identified circa 987 CE (tree-ring age). Although it is possible that this peak is related to a CR event, further investigation of annual  $^{14}\text{C}$  or  $^{10}\text{Be}$  data is needed to support this conclusion.

## Acknowledgments

The authors thank Florian Mekhaldi for comments of the NGRIP and NEEM data and Asami Suzuki and Chihiro Mori for supporting a cutting work of ice core. This work was supported by JSPS KAKENHI grants JP16H06005 and 25247082. The DF  $^{10}\text{Be}$  data are listed in supporting information, and  $\text{Na}^+$  data can be downloaded at <https://ads.nipr.ac.jp/dataset/A20181211-001>.

## References

- Abreu, J. A., Beer, J., Steinhilber, F., Christl, M., & Kubik, P. W. (2013).  $^{10}\text{Be}$  in ice cores and  $^{14}\text{C}$  in tree rings: Separation of production and climate effects. *Space Science Reviews*, 176(1–4), 343–349. <https://doi.org/10.1007/s11214-011-9864-y>
- Baroni, M., Bard, E., Petit, J. R., Magand, O., & Bourlès, D. (2011). Volcanic and solar activity, and atmospheric circulation influences on cosmogenic  $^{10}\text{Be}$  fallout at Vostok and Concordia (Antarctica) over the last 60 years. *Geochimica et Cosmochimica Acta*, 75(22), 7132–7145. <https://doi.org/10.1016/j.gca.2011.09.002>
- Beer, J., McCracken, K., & von Steiger, R. (2012). *Cosmogenic radionuclide theory in the terrestrial and space environments*. Berlin: Springer.
- Büntgen, U., Wacker, L., Galván, J. D., Arnold, S., Arseneault, D., Baillie, M., et al. (2018). Tree rings reveal globally coherent signature of cosmogenic radiocarbon events in 774 and 993 CE. *Nature Communications*, 9(1), 3605. <https://doi.org/10.1038/s41467-018-06036-0>
- Fogtmann-Schulz, A., Østbø, S. M., Nielsen, S. G. B., Olsen, J., Karoff, C., & Knudsen, M. F. (2017). Cosmic ray event in 994 C.E. recorded in radiocarbon from Danish oak. *Geophysical Research Letters*, 44, 8621–8628. <https://doi.org/10.1002/2017GL074208>
- Fourré, E., Jean-Baptiste, P., Dapoigny, A., Baumier, D., Petit, J. R., & Jouzel, J. (2006). Past and 20 recent tritium levels in Arctic and Antarctic polar caps. *Earth and Planetary Science Letters*, 245(1–2), 56–64. <https://doi.org/10.1016/j.epsl.2006.03.003>
- Fujita, S., Holmlund, P., Andersson, I., Brown, I., Enomoto, H., Fujii, Y., et al. (2011). Spatial and temporal variability of snow accumulation rate on the East Antarctic ice divide between Dome Fuji and EPICA DMLK. *The Cryosphere*, 5(4), 1057–1081. <https://doi.org/10.5194/tc-5-1057-2011>

- Güttler, D., Adolphi, F., Beer, J., Bleicher, N., Boswijk, G., Christl, M., et al. (2015). Rapid increase in cosmogenic  $^{14}\text{C}$  in AD 775 measured in New Zealand kauri trees indicates short-lived increase in  $^{14}\text{C}$  production spanning both hemispheres. *Earth and Planetary Science Letters*, *411*, 290–297. <https://doi.org/10.1016/j.epsl.2014.11.048>
- Heikkilä, U., Beer, J., Abreu, J. A., & Steinhilber, F. (2013). On the atmospheric transport and deposition of the cosmogenic radionuclides ( $^{10}\text{Be}$ ): A review. *Space Science Reviews*, *176*(1–4), 321–332. <https://doi.org/10.1007/s11214-011-9838-0>
- Horiuchi, K., Ohta, A., Uchida, T., Matsuzaki, H., Shibata, Y., & Motoyama, H. (2007). Concentration of  $^{10}\text{Be}$  in an ice core from the Dome Fuji station, Eastern Antarctica: Preliminary results from 1500–1810 yr AD. *Nuclear Instruments and Methods in Physics Research Section B: Beam Interactions with Materials and Atoms*, *259*(1), 584–587. <https://doi.org/10.1016/j.nimb.2007.01.306>
- Horiuchi, K., Uchida, T., Sakamoto, Y., Ohta, A., Matsuzaki, H., Shibata, Y., & Motoyama, H. (2008). Ice core record of  $^{10}\text{Be}$  over the past millennium from Dome Fuji, Antarctica: A new proxy record of past solar activity and a powerful tool for stratigraphic dating. *Quaternary Geochronology*, *3*(3), 253–261. <https://doi.org/10.1016/j.quageo.2008.01.003>
- Igarashi, M., Nakai, Y., Motizuki, Y., Takahashi, K., Motoyama, H., & Makishima, K. (2011). Dating of the Dome Fuji shallow ice core based on a record of volcanic eruptions from AD 1260 to AD 2001. *Polar Science*, *5*(4), 411–420. <https://doi.org/10.1016/j.polar.2011.08.001>
- Jull, A. J. T., Panyushkina, I. P., Lange, T. E., Kukarskih, V. V., Myglan, V. S., Clark, K. J., et al. (2014). Excursions in the  $^{14}\text{C}$  record at A.D. 774–775 in tree rings from Russia and America. *Geophysical Research Letters*, *41*, 3004–3010. <https://doi.org/10.1002/2014GL059874>
- Kawamura, K., Abe-Ouchi, A., Motoyama, H., Ageta, Y., Aoki, S., Azuma, N., et al. (2017). State dependence of climatic instability over the past 720,000 years from Antarctic ice cores and climate modeling. *Science Advances*, *3*(2), e1600446. <https://doi.org/10.1126/sciadv.1600446>
- Matsuzaki, H., Nakano, C., Tsuchiya, Y., Kato, K., Maejima, Y., Miyairi, Y., et al. (2007). Multi-nuclides AMS performances at MALT. *Nuclear Instruments and Methods in Physics Research Section B Beam Interactions with Materials and Atoms*, *259*(1), 36–40. <https://doi.org/10.1016/j.nimb.2007.01.145>
- Mekhaldi, F., Muscheler, R., Adolphi, F., Aldahan, A., Beer, J., McConnell, J. R., et al. (2015). Multiradionuclide evidence for the solar origin of the cosmic-ray events of AD 774/5 and 993/4. *Nature Communications*, *6*(1), 8611. <https://doi.org/10.1038/ncomms9611>
- Miyake, F., Masuda, K., Hakozaiki, M., Nakamura, T., Tokanai, F., Kato, K., et al. (2014). Verification of the cosmic ray event in AD 993–994 by using a Japanese Hinoki tree. *Radiocarbon*, *56*(03), 1189–1194. <https://doi.org/10.2458/56.17769>
- Miyake, F., Masuda, K., & Nakamura, T. (2013). Another rapid event in the carbon-14 record of tree rings. *Nature Communications*, *4*(1), 1748. <https://doi.org/10.1038/ncomms2873>
- Miyake, F., Nagaya, K., Masuda, K., & Nakamura, T. (2012). A signature of cosmic-ray increase in AD 774–775 from tree rings in Japan. *Nature*, *486*(7402), 240–242. <https://doi.org/10.1038/nature11123>
- Miyake, F., Suzuki, A., Masuda, K., Horiuchi, K., Motoyama, H., Matsuzaki, H., et al. (2015). Cosmic ray event of A.D. 774–775 shown in quasi-annual  $^{10}\text{Be}$  data from the Antarctic Dome Fuji ice core. *Geophysical Research Letters*, *42*, 84–89. <https://doi.org/10.1002/2014GL062218>
- Motizuki, Y., Motoyama, H., Nakai, Y., Suzuki, K., Iizuka, Y., & Takahashi, K. (2017). Overview of the chemical composition and characteristics of  $\text{Na}^+$  and  $\text{Cl}^-$  distributions in shallow samples from Antarctic ice core DF01 (Dome Fuji) drilled in 2001. *Geochemical Journal*, *51*(3), 293–298. <https://doi.org/10.2343/geochemj.2.0458>
- Motizuki, Y., Nakai, Y., Takahashi, K., Igarashi, M., Motoyama, H., & Suzuki, K. (2014). Dating of a Dome Fuji (Antarctica) shallow ice core by volcanic signal synchronization with B32 and EDML1 chronologies. *The Cryosphere Discussions*, *8*(1), 769–804. <https://doi.org/10.5194/tcd-8-769-2014>
- Park, J., Southon, J., Fahrni, S., Creasman, P. P., & Mewaldt, R. (2017). Relationship between solar activity and  $\Delta^{14}\text{C}$  peaks in AD 775, AD 994, and 660 BC. *Radiocarbon*, *59*(04), 1147–1156. <https://doi.org/10.1017/RDC.2017.59>
- Polunianov, S. V., Kovaltsov, G. A., Mishev, A. L., & Usoskin, I. G. (2016). Production of cosmogenic isotopes  $^7\text{Be}$ ,  $^{10}\text{Be}$ ,  $^{14}\text{C}$ ,  $^{22}\text{Na}$ , and  $^{36}\text{Cl}$  in the atmosphere: Altitudinal profiles of yield functions. *Journal of Geophysical Research: Atmospheres*, *121*, 8125–8136. <https://doi.org/10.1002/2016JD025034>
- Rakowski, Z., Krapiec, M., Huels, M., Pawlyta, J., Dreves, A., & Meadows, J. (2015). Increase of radiocarbon concentration in tree rings from Kujawy (SE Poland) around AD 774–775. *Nuclear Instruments and Methods in Physics Research B*, *361*, 564–568. <https://doi.org/10.1016/j.nimb.2015.03.035>
- Sigl, M., Winstrup, M., McConnell, J. R., Welten, K. C., Plunkett, G., Ludlow, F., et al. (2015). Timing and climate forcing of volcanic eruptions for the past 2,500 years. *Nature*, *523*(7562), 543–549. <https://doi.org/10.1038/nature14565>
- Steinhilber, F., Abreu, J. A., Beer, J., Brunner, I., Christl, M., Fischer, H., et al. (2012). 9,400 years of cosmic radiation and solar activity from ice cores and tree rings. *Proceedings of the National Academy of Sciences of the United States of America*, *109*(16), 5967–5971. <https://doi.org/10.1073/pnas.1118965109>
- Stuiver, M., Reimer, P. J., Bard, E., Beck, J. W., Burr, G. S., Hughen, K. A., et al. (1998). INTCAL98 radiocarbon age calibration, 24,000-0 cal BP. *Radiocarbon*, *40*(3), 1041–1083. <https://doi.org/10.1017/S0033822200019123>
- Sukhodolov, T., Usoskin, I., Rozanov, E., Asvestari, E., Ball, W. T., Curran, M. A. J., et al. (2017). Atmospheric impacts of the strongest known solar particle storm of 775 AD. *Scientific Reports*, *7*(1), 45257. <https://doi.org/10.1038/srep45257>
- Uemura, R., Motoyama, H., Masson-Delmotte, V., Jouzel, J., Kawamura, K., Goto-Azuma, K., et al. (2018). Asynchrony between Antarctic temperature and  $\text{CO}_2$  associated with obliquity over the past 720,000 years. *Nature Communications*, *9*(1), 961. <https://doi.org/10.1038/s41467-018-03328-3>
- Usoskin, I. G., & Kovaltsov, G. A. (2012). Occurrence of extreme solar particle events: Assessment from historical proxy data. *The Astrophysical Journal*, *757*(1), 92. <https://doi.org/10.1088/0004-637X/757/1/92>
- Usoskin, I. G., & Kromer, B. (2005). Reconstruction of the  $^{14}\text{C}$  production rate from measured relative abundance. *Radiocarbon*, *47*(01), 31–37. <https://doi.org/10.1017/S0033822200052176>
- Usoskin, I. G., Kromer, B., Ludlow, F., Beer, J., Friedrich, M., Kovaltsov, G. A., et al. (2013). The AD775 cosmic event revisited: The Sun is to blame. *Astronomy and Astrophysics*, *552*, L3. <https://doi.org/10.1051/0004-6361/201321080>
- Uusitalo, J., Arppe, L., Hackman, T., Helama, S., Kovaltsov, G., Mielikäinen, K., et al. (2018). Solar superstorm of AD 774 recorded sub-annually by Arctic tree rings. *Nature Communications*, *9*(1), 3495. <https://doi.org/10.1038/s41467-018-05883-1>
- Wagner, G., Masarik, J., Beer, J., Baumgartner, S., Imboden, D., Kubik, P. W., et al. (2000). Reconstruction of the geomagnetic field between 20 and 60 kyr BP from cosmogenic radionuclides in the GRIP ice core. *Nuclear Instruments and Methods in Physics Research*, *172*(1–4), 597–604. [https://doi.org/10.1016/S0168-583X\(00\)00285-8](https://doi.org/10.1016/S0168-583X(00)00285-8)